New Journal of Physics
The open access journal at the forefront of physics

Deutsche Physikalische Gesellschaft DPG IOP Institute of Physics

PAPER • OPEN ACCESS

Robust polarization gradient cooling of trapped ions

To cite this article: Wenbing Li *et al* 2022 *New J. Phys.* **24** 043028

New Journal of Physics
The open access journal at the forefront of physics

Deutsche Physikalische Gesellschaft DPG
IOP Institute of Physics

Published in partnership with: Deutsche Physikalische Gesellschaft and the Institute of Physics

OPEN ACCESS

RECEIVED
3 September 2021

REVISED
25 March 2022

ACCEPTED FOR PUBLICATION
29 March 2022

PUBLISHED
21 April 2022

PAPER

Robust polarization gradient cooling of trapped ions

Wenbing Li[1,2,*], **Sebastian Wolf**[1,*], **Lukas Klein**[1], **Dmitry Budker**[1,2,3,4], **Christoph E Düllmann**[2,3,5,6] **and Ferdinand Schmidt-Kaler**[1,2]

[1] QUANTUM, Institut für Physik, Johannes Gutenberg-Universität Mainz, 55128 Mainz, Germany
[2] Helmholtz-Institut Mainz, 55099 Mainz, Germany
[3] PRISMA Cluster of Excellence, Johannes Gutenberg-Universität Mainz, 55128 Mainz, Germany
[4] Department of Physics, University of California, Berkeley, CA 94720-7300, United States of America
[5] Department Chemie, Johannes Gutenberg-Universität Mainz, 55128 Mainz, Germany
[6] GSI Helmholtzzentrum für Schwerionenforschung GmbH, 64291 Darmstadt, Germany
[*] Authors to whom any correspondence should be addressed.

E-mail: wenbingli@uni-mainz.de and wolfs@uni-mainz.de

Keywords: trapped ions, laser cooling, sub-Doppler cooing, polarization gradient cooling

Abstract

We implement three-dimensional polarization gradient cooling (PGC) of trapped ions. Counter-propagating laser beams near 393 nm impinge in lin $\perp$ lin configuration, at a frequency below the $S_{1/2}$ to $P_{3/2}$ resonance in $^{40}Ca^{+}$. Our measurements demonstrate that cooling with laser beams detuned to lower frequencies from the resonance is robust against an elevated phonon occupation number and works continuously in the crossover from regular Doppler cooling to detunings of tens of linewidths. It is thus robust against heating events and also works well for an initial ion motion far out of the Lamb–Dicke regime. We show that PGC performance strongly depends on residual micromotion (MM) and find PGC working for a MM modulation index $\beta \leqslant 0.1$. Still, we find that the spectral impurity of the laser field affects both, cooling rates and cooling limits. Thus, a Fabry–Pérot cavity filter is employed to efficiently suppress amplified spontaneous emission of the diode laser. We demonstrate mean phonon numbers for a single ion of 5.4(4) at a trap frequency of $2\pi \times 285$ kHz and 3.3(4) at $2\pi \times 480$ kHz, in the axial and radial directions, respectively.

1. Introduction

Laser-cooled trapped ions are widely used in quantum simulation [1–3] and quantum computation [4–6], for high-performance optical clocks [7–10] or precision spectroscopy [11–15]. For those applications, Coulomb crystals are formed under Doppler cooling [16–18]. However, in order to improve the fidelity of quantum gate operations in an ion-based quantum computer, to reduce systematic errors in an optical ion clock, and in precision spectroscopy applications, one may require deeper cooling of the ion degrees of motion, including collective modes in the ion crystal.

Nearly perfect ground state cooling is routinely achieved by resolved sideband (SB) cooling techniques which either employ a narrow dipole-forbidden transition [19–21] or Raman transitions between hyperfine or Zeeman ground state levels [22–24]. For a crystal of N ions, the number of collective modes is $3N$ such that sequentially cooling on all resolved SBs becomes increasingly impractical for large N. However, the spectral lineshape of a three-level system may be tailored by electromagnetically induced transparency (EIT) such that multiple collective modes are cooled simultaneously [25–28]. This bandwidth of cooling—well suited to cool a collection of collective modes—may be further increased in the polarization gradient cooling (PGC) method. In the pioneering theoretical work by Cohen-Tannoudji and co-workers [29, 30], sub-Doppler PGC experimental results on atomic ensembles obtained by Chu, Phillips *et al* were explained, for which all three were awarded the Physics Nobel prize in 1997 [31–33]. Also for trapped ions, sub-Doppler cooling was proposed [34, 35] and led to first experiments by PGC [36]. Recently, PGC was

demonstrated for a single trapped ion in three dimensions, and for small linear crystals [37], highlighting the large cooling bandwidth of this method. PGC was extended to linear ion crystals with up to 51 ions and 2D-crystals in zigzag configuration with 22 ions along a single trap axis [38].

The most appealing application of PGC is sub-Doppler multi-mode cooling over a large band of motional frequencies. The PGC cooling bandwidth exceeds that of EIT cooling, leading to a fast reduction of phonon numbers even for a large number of vastly different mode frequencies, significantly below Doppler cooling limits. In this work, we implement 3D PGC with red detuning (the laser frequency below resonance of the dipole transition $S_{1/2} \leftrightarrow P_{3/2}$ near 393 nm in singly charged $^{40}Ca^{+}$). This technique demonstrates robust sub-Doppler cooling for trapped ions far beyond Lamb–Dicke regime (LDR). We investigate, for the first time, the residual micromotion (MM) is a significant effect on PGC, which is only accessible when employing beams with a nonvanishing projection on the radial direction of the Paul trap. We find that the red detuning allows us to implement PGC even with excessively high initial phonon numbers, orders of magnitude above that which had been reported so far. In this configuration, using red detuned light fields, PGC does not require Doppler precooling anymore. In addition, PGC with red detuned light allows us to study the crossover between PGC and Doppler cooling, e.g. to optimize the cooling rate. With small frequency detuning, the parasitic Doppler heating of the lights for PGC that also can work for Doppler cooling is reduced during PGC, which is especially important for fast PGC with light detuned by only a few linewidths of $2\pi \times 23$ MHz from the dipole transition. Such robust PGC may be advantageous in case of non-ideal Doppler precooling or if the ions are exposed to strong heating events. We see an application case for externally generated (exotic) ions, injected into a Paul trap, captured and then sympathetically cooled down and incorporated into a laser-cooled host ion crystal. Specifically, we aim for precision spectroscopy of injected ions of various thorium isotopes and the low-energy isomer in ^{229}Th [39–42].

The paper is organized as follows: we start describing the PGC scheme in section 2 and the ion trap and laser experimental setup in section 3. And then present the PGC cooling results for a single ion and for a four-ion linear crystal. Furthermore, we study the robustness of PGC in typically encountered experimental situations such as excessively high initial phonon occupation number, an imperfect localization of the ion position at the trap center in section 4. We investigate the laser sources for PGC with spectral impurity in section 5. This results demonstrate PGC as a versatile method for preparing ions in low axial and radial vibrational states.

2. Levels and transitions for PGC in $^{40}Ca^{+}$

Levels and relevant transitions in $^{40}Ca^{+}$ are shown in figure 1(a) and the most important transition for PGC near 393 nm with its Zeeman components in figure 1(b). The dipole-allowed transition from $S_{1/2}$ to $P_{3/2}$ is excited off-resonantly by a pair of counter-propagating 393 nm beams in lin $\perp$ lin configuration, forming thus a periodically varying spatial polarization gradient lattice along this direction with alternating $\sigma^{+}, \pi, \sigma^{-}, \pi, \ldots$etc polarization. If the frequency is red detuned relative to the $S_{1/2}$ to $P_{3/2}$ transition by Δ, the variation of the Clebsch–Gordan coefficients leads to a periodically varying ac-Stark shift of the ground state Zeeman sublevels [31, 33], as shown in figure 1(c). If the ion moves along the direction of this lattice, predominantly either $m_J = +1/2 \leftrightarrow m_J = +3/2$ or $m_J = -1/2 \leftrightarrow m_J = -3/2$ transitions are alternately excited, in spatial regions with polarization of either σ^{+} or σ^{-}, respectively. From the combination of ac-light shift and optical pumping, the ion will lose kinetic energy when climbing a potential hill. The wave vectors of the PGC beams are parallel with the magnetic field B. Its projections with the trap directions (x, y, z) have angles (60°, 60°, 45°) as shown in figure 1(d). Thus, in this setting PGC is acting in all three dimensions, and cools axial and radial modes of vibration. The magnetic field strength of $\approx$343 μT is supplied with a set of permanent magnets which defines the quantization axis and leads to a splitting of $2\pi \times 9.343$ MHz between the two Zeeman sublevels of the $S_{1/2}$ manifold.

Calcium atoms evaporated from an oven are photoionized resonantly in two photons step scheme with beams at wavelength of 423 nm and 375 nm and captured in the trap. For Doppler cooling, 397 nm light is red detuned from the dipole-allowed $S_{1/2}$ to $P_{1/2}$ transition by $\Delta \simeq -0.5\Gamma$. Pumping out of the metastable D states is accomplished with beams near 866 nm and 854 nm. A beam near 729 nm is aligned parallel to the magnetic field direction and used for resolved SB spectroscopy driving the narrow quadrupole $|S_{1/2}, m_J = 1/2\rangle \leftrightarrow |D_{5/2}, m_J = 3/2\rangle$ transition for revealing the ion phonon mode occupation numbers.

3. Experimental setup and procedures

We designed and built a linear Paul trap with blade-shaped radio frequency (RF) and DC (static voltage) electrodes which are integrally machined out of one piece of stainless-steel. The RF electrodes feature a

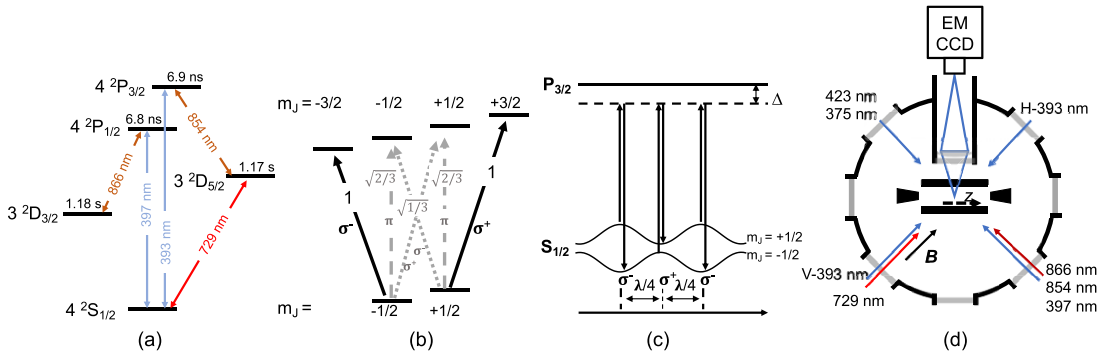

Figure 1. (a) Levels and relevant transitions and lifetimes in $^{40}Ca^{+}$. (b) Energy levels and transitions involved in PGC. A static magnetic field yields a Zeeman splitting of $2\pi \times 9.343$ MHz in the ground $S_{1/2}$ state. The Clebsch–Gordan coefficients are shown for the transitions indicated with arrows. (c) Spatially varying light polarization results in position-dependent light shifts. The frequency of the PGC laser beams near 393 nm is detuned by Δ from the $S_{1/2} \leftrightarrow P_{3/2}$ transition, and the wave vector **k** of both counter-propagating beams is aligned parallel to the magnetic field. (d) Geometry of trap, laser beams and magnetic field **B**. The counter-propagating PGC beams are polarized horizontally (H-) and vertically (V-). Laser beams near 423 nm and 375 nm serve for photoionization loading, laser beams near 397 nm, 866 nm, 854 nm are used for Doppler cooling, and the ion fluorescence is imaged on a electron multiplying charge-coupled device (EMCCD) camera. Light tuned near 729 nm is employed for resolved SB spectroscopy.

distance of 2 mm from the trap center. We operate the trap at RF frequency $\Omega = 2\pi \times 5.83$ MHz with a peak-to-peak amplitude of 550 V to the RF pair of electrodes and generate trap frequencies of $(\omega_x, \omega_y) = 2\pi \times (483, 480)$ kHz for the two radial directions. The DC pair is grounded, or kept at a small ($<$10 V) voltage lifting further the degeneracy between radial trap frequencies. The axial confinement is provided by two end-cap electrodes at 14 mm distance. For a DC voltage of +800 V, an axial frequency $\omega_z = 2\pi \times 220$ kHz is created along the z-direction of the trap.

The laser system used in the experiment includes external-cavity diode lasers[7] operating near 397 nm for Doppler cooling, 866 nm and 854 nm for repumping, and 393 nm for PGC lattice. In addition, 729 nm light for probing the narrow quadrupole transition is supplied with a DL TA pro (tapered amplifier) locked to a high finesse optical cavity via Pound–Drever–Hall resulting in a short-term frequency instability of $\leqslant$100 Hz. The laser beams are switched by acousto-optic modulators operated in double pass configuration. All laser beams are coupled to the setup via polarization-maintaining single-mode fibers to ensure alignment stability. Laser-induced ion fluorescence is collected with a lens and imaged at a magnification of $\approx$11.3 onto an EMCCD camera.

We investigate PGC with the following experimental sequence. First, the Ca ions are Doppler cooled with 397 nm laser light for 5 ms. The repumping light at 866 nm is switched on during Doppler cooling to prevent accumulation of ions in the $D_{3/2}$ state. Second, the PGC laser beams at 393 nm are applied to the ions at orthogonal linear polarization and along the magnetic field. The two beams have a frequency difference of 50 kHz to create a moving polarization gradient. This is needed so that all ion wave packets experience a significant polarization gradient lattice at some point during the PGC period. This should not be necessary for ion wave packets that are larger than a period of the gradient; our experimental situation corresponds to the borderline of this regime. We started with a value that is smaller than the axial trap frequency. After that, we tried to optimize the value by checking the final phonon number with different frequencies. However, we did not find that there was significant dependence even down to zero frequency difference. We conjecture that this is due the inherent phase fluctuations on both light paths of length $\sim$1.2 m. The intensity of the two 393 nm laser beams are calibrated with the fluorescence intensity detected with the EMCCD camera. During a PGC period, the light at 866 nm and at 854 nm is switched on to pump the populations out of the $D_{3/2}$ and $D_{5/2}$ states. Third, the ions are prepared in the $|S_{1/2}, m_J = 1/2\rangle$ state via frequency-resolved optical pumping on the $|S_{1/2}, m_J = -1/2\rangle \leftrightarrow |D_{5/2}, m_J = 1/2\rangle$ transition by a laser pulse at 729 nm combined with light at 854 nm. Finally, the motional state is probed by addressing the carrier and first-order SB of the $|S_{1/2}, m_J = 1/2\rangle \leftrightarrow |D_{5/2}, m_J = 3/2\rangle$ transition with a 729 nm laser pulse. At the end, the quantum state is read out for all individual ions via spatially resolved fluorescence detection at 397 nm recorded with the EMCCD camera. In this work, the ions is outside the LDR such that we cannot extract the phonon number from the SBs spectra since the sizable asymmetry cannot be observed even after PGC. Therefore, the final phonon number is determined by fitting the Rabi oscillations of the carrier and first order blue and red SBs for the single ion, and in the same way for the multi-ion crystals.

[7] All lasers are TOPTICA DL pro.

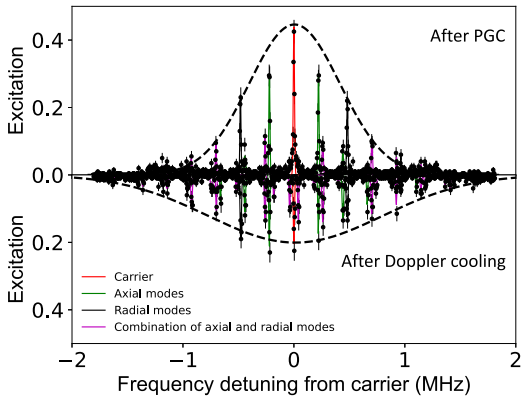

Figure 2. Spectra of motional states. The $|S_{1/2}, m_J = 1/2\rangle \leftrightarrow |D_{5/2}, m_J = 3/2\rangle$ transition is probed with a laser pulse at 729 nm after PGC (top) and after Doppler cooling (bottom). Each experimental point (black solid circles) is the average of 200 measurements. The envelope fit (dashed black lines) include all the SBs by taking into account the maxima of Gaussian fits to the carrier transition (red), axial SBs (green), radial SBs (black solid line) and combinations of axial and radial SBs (magenta).

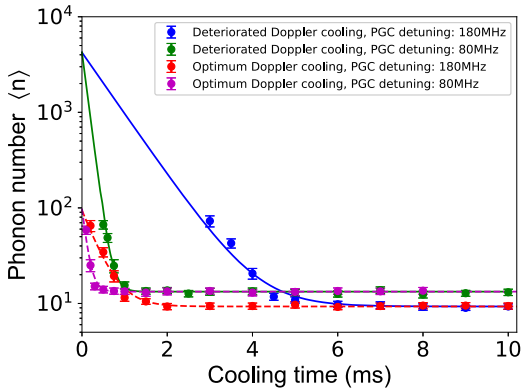

Figure 3. PGC performance for different cooling times and different initial phonon numbers. The initial state is prepared by Doppler cooling, which is either optimized or deliberately spoiled by tuning the Doppler cooling light close to resonance ($\Delta \ll \Gamma$). The characteristic cooling times are $\lesssim$7.0 ms (blue circles fit with dashed line) and $\lesssim$1.5 ms (green) and the final mean phonon numbers 9.3(7) and 13.3(11), for PGC-light detuning of $2\pi \times 180$ MHz and $2\pi \times 80$ MHz, respectively. With low initial phonon numbers, the cooling times are decreased to $\lesssim$3.0 ms (red) and $\lesssim$0.75 ms (magenta), respectively. The data in this figure were taken without the cavity filter.

4. Experimental characterization of PGC

Three dimensional PGC is compared to Doppler cooling on a single Ca^+ ion by SB spectroscopy of the $|S_{1/2}, m_J = 1/2\rangle \leftrightarrow |D_{5/2}, m_J = 3/2\rangle$ transition, as shown in figure 2. In this measurement, the 393 nm laser light is red-detuned by $2\pi \times 180$ MHz, as determined with a wavelength meter[8]. The intensity of the 729 nm light for both measurements is same. The SB data are fitted with individual Gaussian profiles. The higher-order SBs involving the axial and radial motional modes and the higher order SBs are considerably suppressed for the PGC case. Furthermore, a Gaussian envelope fit to the SB amplitudes reveals a linewidth for the PGC case reduced by a factor of 1.92(6) compared to that with Doppler cooling.

To investigate the robustness of the presented PGC method, we initialize the ion with high initial phonon number occupation (>4000 phonons, extracted from the extrapolated logarithmic fit in figure 3) by artificially deteriorating Doppler cooling via detuning the 397 nm light close to resonance ($\Delta \ll \Gamma$) of the $S_{1/2}$ to $P_{1/2}$ transition. The cooling results compared with PGC after optimal Doppler cooling are shown in figure 3. With sufficient cooling time, identical final mean phonon numbers can be achieved independent of the initial ion temperature. For a detuning of $2\pi \times 180$ MHz, the equilibrium cooling time is more than twice as long for high initial phonon numbers as for low initial phonon numbers. The PGC time can be reduced by decreasing the detuning of PGC light to $2\pi \times 80$ MHz, which in turn increases the scattering rate of PGC light. We have also realized PGC for detunings as small as 30 MHz, and this was decreasing the

[8] WS7, HighFinesse.

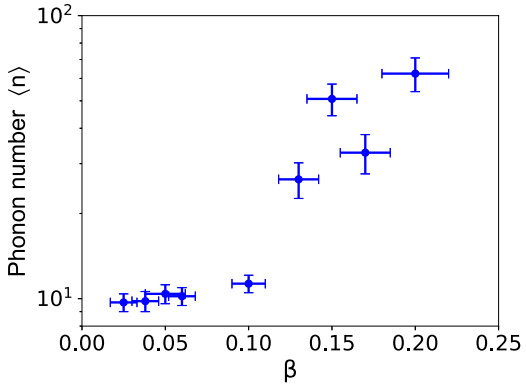

Figure 4. Mean phonon numbers with the transition coupling strength on the MM SB. The residual MM is changed by scanning the compensation voltages in one of the radial directions. The performance of PGC drops significantly for a modulation index $\beta > 0.1$.

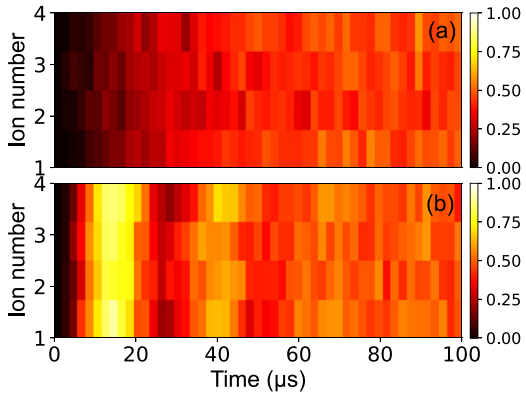

Figure 5. Rabi dynamics for a four-ion linear crystal recorded individually on the carrier transition with an axial trap frequency of 190 kHz. For Doppler cooled ions (a), no oscillations are visible, while they can clearly be observed after PGC (b).

cooling time to $\leqslant 35$ μs at the price of an elevated mean phonon number. With this small detuning of 30 MHz, the cooling time is decreased about two orders of magnitude compared with the optimum configuration shown in figure 3. However, the final phonon numbers are just about half Doppler cooing limit. For red-detuned PGC, we can explore the cross-over to Doppler cooling.

For three-dimensional PGC, residual MM as one of the crucial heating sources for trapped ions is detrimental, especially for weak radial trap potentials. Therefore, we also investigate the influence of MM on PGC by adjusting MM-compensation voltages. The MM modulation index β is determined from the ratio of the excitation strength at the carrier and the MM-SB frequency. We find PGC to be robust against residual MM corresponding to a range where the MM-compensation DC voltage is changed by 1.6 V (corresponding to a displacement of 560(35) nm from the trap center) and thus a MM-modulation index $\beta \leqslant 0.1$, see figure 4. However, MM is a decisive factor for three dimensional PGC. Therefore, the residual MM has to be compensated within a proper range. Otherwise, the ions will be heated up during the cooling time duration of PGC.

We extend PGC to a four-ion linear crystal confined in a trap potential, where the radial trap frequencies degeneracy is lifted by applying 3.0 V on the DC electrode pair. The trap frequencies are $(\omega_x, \omega_y, \omega_z) = 2\pi \times (427, 505, 190)$ kHz. The optical parameters used here are the same as the optimized for a single ion. We determine the axial phonon number by measuring Rabi oscillations on the $S_{1/2} \leftrightarrow D_{5/2}$ transition. The Rabi oscillations of all four ions on the carrier transition are recorded individually to demonstrate the improved cooling of PGC with respect to Doppler cooling as shown in figure 5. For the Doppler-cooled ion crystal, no Rabi oscillations are visible for low trap frequencies, as shown in figure 5(a). This is due to the averaging of Rabi oscillations for different phonon numbers, coined spectator modes effect [43]. However, for the PGC case, Rabi oscillations can be explicitly observed, see figure 5(b). Since all motional modes contribute to the Rabi dynamics of the carrier transition, this result indicates a low phonon occupation number for each motional mode of the four-ion linear crystal. In contrast to the previous work [38] our experimental geometry allows for addressing all 3D motional modes. Having a projection on the

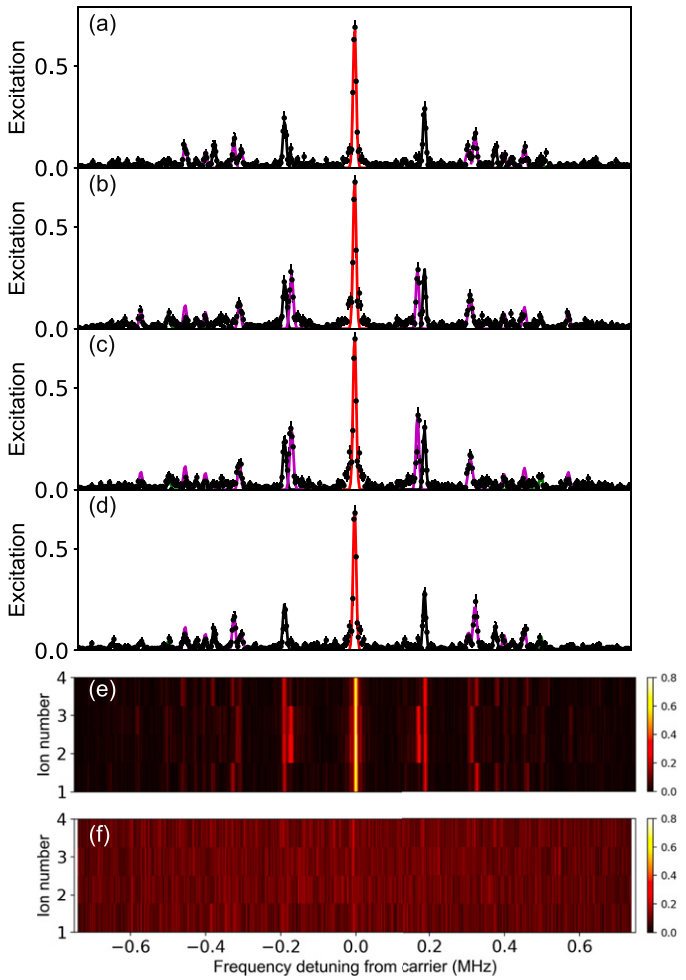

Figure 6. Sideband spectra of a four-ion linear crystal after PGC recorded on individual ions display carrier and SB, depending on the site in the crystal (a)–(d), see inset with eigenvectors of different length for the axial modes. We fit Gaussian profiles to the data: carrier (red line), and axial modes (black lines), and the mixing between the radial COM and the first breathing mode at 505 kHz−330 kHz = 175 kHz (magenta). Note, that this resonance only appears for central ions (a) and (d) with a strong first breathing eigenvector. In contrast, the fourth axial mode at 582 kHz is only excited sufficiently strong on the innermost ions (b) and (c). Each experimental point (black solid circles) is the average of 200 measurements. Note, that for the central ions in the crystal, the first breathing mode is suppressed, while the fourth mode is suppressed for the outer ions. In the density plot the difference between PGC (e) and Doppler cooling (f) is clarified, as in the latter case SBs are washed out.

radial modes also allows for studying the PG cooling of all modes, see figure 2. Also, the effect of a MM compensation on PGC can be studied in this geometry, because radial MM is typically much larger as compared to the axial one.

The individual motional modes of the four-ion linear crystal are investigated with spatially resolved SB spectroscopy, as shown in figure 6. All the SBs including center-of-mass (COM) and breathing modes of four ions can be distinctly resolved after PGC as shown in figures 6(a)–(e). In contrast, for the Doppler cooled case shown in figure 6(f) the high phonon numbers for each motional mode, and therefore the emergence of higher harmonics, prevent the resolution of individual SBs. The final mean phonon number of the axial mode is evaluated as 12.5(7) after PGC by measuring Rabi oscillations of the carrier transition and the first axial SBs of the COM mode of the inner ions.

5. Technique for improving PGC efficiency

An external-cavity diode laser is used for PGC in this work. In this case, resonant scattering events due to the amplified spontaneous emission (ASE) of the laser diode represent an additional heating source. The final temperature after PGC would be limited by this effect, especially if the frequency detuning is increased in order to approach the theoretical temperature limit [33, 38]. For large detunings, the lower cooling rate will be surpassed by the heating rate of the ASE background. To investigate this regime, we build a Fabry–Pérot cavity to purify the laser spectrum. Two mirrors with reflectivity of 99(1)% are spaced by 8 cm to form an optical resonator with a free spectral range of 1.87 GHz and a finesse of about $\mathscr{F} = 310$. The

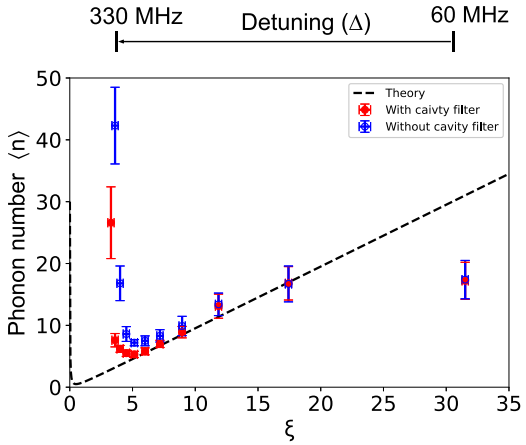

Figure 7. Mean phonon number after PGC for different $\xi = s\Delta/(3\omega_z)$, realized by changing the detuning Δ with (red solid circles) and without (blue hollow circles) spectral purification via the cavity filter, respectively. The minimum mean phonon number at a detuning of $2\pi \times 210$ MHz is reduced by 2.0(3) phonons. The dashed line indicates the theoretical predicted mean phonon number with ξ.

measured extinction of ASE is in good agreement with the expected value of $(1-R)^2 \approx 10^{-4}$. To stabilize the cavity and power of the transmitted light, the cavity is frequency locked at low Fourier frequencies to the 393 nm laser by a piezo-transducer. The 393 nm laser is frequency locked at high Fourier frequencies to the cavity by the laser current which makes the laser frequency can follow the cavity quickly. At the same time, the 393 nm laser frequency is kept stable using feedback from the high precision wavelength meter WS07. The resulting cavity filter with linewidth $\Delta\nu \approx 6$ MHz, consequently, is able to sufficiently suppress spectral impurities of the laser light.

In an ideal case, the final mean phonon number is expected to be $\langle n_0(\xi)\rangle = \xi + 1/(4\xi) - 1/2$ for a single ion [38], where $\xi = s\Delta/(3\omega_z)$ is a dimensionless parameter, Δ is the frequency detuning of 393 nm light, and ω_z is the trap frequency in the axial direction. The saturation parameter is defined as $s = \frac{\Omega^2/2}{\Gamma^2/4+\Delta^2}$, with $\Gamma = 2\pi \times 23$ MHz the width of the excited state $P_{3/2}$ and Ω the Rabi frequency. To investigate how well we approach this limit using light with purified spectrum we measure the final mean phonon number for different frequency detunings of the 393 nm light with fixed power. For this experiment, the trap frequencies are $(\omega_x, \omega_y, \omega_z) = 2\pi \times (483, 480, 285)$ kHz. Figure 7 shows the results with (red) and without (blue) cavity filter, respectively, and the theory fit with the laser intensity as the free parameter. Suggests that theoretical estimation a minimum mean phonon number of $1/2$ can be achieved for $\xi = 1/2$ when the optical well depth $(2s\Delta/3)$ equals the trap frequency ω_z. From our measurement, the phonon number is in agreement with the theory prediction for $\xi > 5$. However, the minimum phonon number $1/2$ predicted by the theory cannot be reached in our experiment since the trap potential is weak. Indeed, when the detuning is decreased to reduce the optical potential closer to the theoretical optimum, the optical pumping rate also decreases and, eventually, PGC cannot counteract the trap heating rate. At the frequency detuning of $2\pi \times 210$ MHz, the minimal achieved phonon number is reduced by 2.0(3) when using the cavity filter.

To further investigate the effect of the ASE, we measure the cooling dynamics of PGC with and without cavity filter with a fixed frequency detuning of $2\pi \times 210$ MHz and fixed intensity, see figure 8. The observed cooling time is improved by a factor of 2.1(2). To investigate the resonant scattering rate caused by the ASE we measured the pumping time from the $m_J = +1/2$ Zeeman state to the equilibrium distribution in the ground $S_{1/2}$ state, as follows. After Doppler cooling, the ion is prepared in the $|S_{1/2}, m_J = +1/2\rangle$ ground state via optical pumping with 729 nm and 854 nm laser light. Afterward, the 393 nm laser is applied to the ion with a varying duration resulting in partial population of the $|S_{1/2}, m_J = -1/2\rangle$ level. Finally, the population in the $|S_{1/2}, m_J = +1/2\rangle$ state is shelved to the $D_{5/2}$ level with a 729 nm laser pulse and the residual population in the $|S_{1/2}, m_J = +1/2\rangle$ state is detected by a fluorescence measurement. By scanning the pulse duration of the 393 nm laser light, the time to reach an equilibrium between the Zeeman ground states is measured for different frequency detunings as shown in the inset of figure 8. The increased equilibriation time when the cavity filter is used compared with the case without the cavity filter is a result of reduced ASE background of the diode laser leading to a decreased resonant scattering rate. The suppression of the ASE background of the diode laser by the Fabry–Pérot cavity filter results in a reduced additional heating rate and, therefore, an improved cooling rate and final mean phonon number after PGC. The cavity-filter technique provides an option to improve PGC, even with diode lasers with excessive ASE.

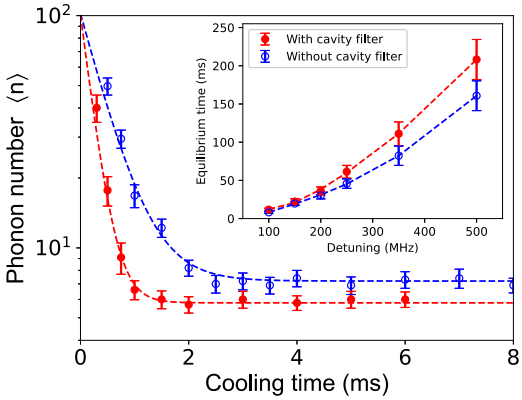

Figure 8. Cooling dynamics of PGC with (red solid circles) and without (blue hollow circles) cavity filter for fixed detuning of $2\pi \times 210$ MHz and fixed intensity of the laser beams. The equilibrium cooling rate is improved by a factor of 2.1(2) when the cavity filter is used. Inset: pumping dynamics from one $S_{1/2}$ Zeeman state to the equilibrium by the 393 nm light beams with (red solid circles) and without (blue hollow circles) cavity filter, respectively. The increased pumping rate without the cavity filter is caused by additional resonant scattering events due to the ASE background.

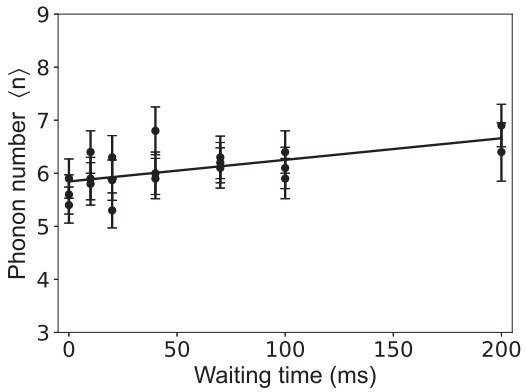

Figure 9. Heating rate of axial motional mode. The mean phonon number is measured for different waiting times after PGC. A linear fit reveals a heating rate of 4.1(8) phonons per second for a trap frequency of $2\pi \times 285$ kHz.

To test whether the ultimate PGC performance would be limited by the heating rate of the trap, we evaluate heating in the axial motional mode. The final mean phonon number is measured for different waiting times after PGC. A linear fit to the data in figure 9 reveals a heating rate of 4.1(8) phonons per second at an axial trap frequency of $2\pi \times 285$ kHz. This rate is of the same order of magnitude as the cooling rate close to final temperatures at the detuning of $2\pi \times 210$ MHz and contributes to the limitation in achievable final mean phonon number of PGC.

6. Conclusion and outlook

We implement three-dimensional PGC for trapped Ca^+ ions in a linear Paul trap with initial temperatures corresponding to ion motion being far outside the LDR. Sideband spectroscopy after PGC shows all motional modes to be well below the Doppler-cooling limit. Efficient cooling close to the ground state even with elevated initial phonon numbers (>4000 phonons) demonstrates the robustness of the presented method. The deterministic influence of residual MM on PGC is discussed. While our results fit well to a rudimentary semiclassical PGC theory, the quantitative comparison in the crossover regime between PGC and Doppler of ion crystals might need a more refined theory development.

We have shown PGC for single ions and extended the cooling technique to linear crystals consisting of four ions reaching a final mean phonon number for the common mode of 12.5(7) at common mode of the axial trap frequency of $2\pi \times 190$ kHz. Furthermore, we find that the spectral impurity of the laser field adversely affects the cooling rate and cooling limit of PGC. Thus, we employ a Fabry–Pérot cavity to suppress ASE of the diode laser. The mean phonon number is improved by 2.0(3) phonons and the cooling time is decreased by a factor of 2.1(2). A mean phonon number limit of 5.4(4) is achieved at a trap

frequency of $2\pi \times 285$ kHz in the axial direction. The heating rate of the trap is estimated to be 4.1(8) phonons per second, which, in combination with the estimates of the cooling rate presented in section 5, indicates that the lowest achievable phonon number is several phonons per mode.

The cavity-filter technique provides an option to improve PGC, even with diode lasers with an ASE component in the emission spectrum. This robust PGC scheme will be extended to larger ion crystals, including 3D formations, and can be beneficial for capturing and sympathetically cooling injected 'impurity' ions, e.g. thorium [39], below the Doppler cooling limit.

Acknowledgments

WL thanks M K Joshi for helpful discussions. We thank Ulrich Poschinger and Daniel Wessel for careful reading and helpful comments. This work was supported in part by the Cluster of Excellence 'Precision Physics, Fundamental Interactions, Structure of Matter' (PRISMA+ EXC 2118/1) and Helmholtz Excellence Network ExNet020, funded by the German Research Foundation (DFG) within the German Excellence Strategy (Project ID 39083149), the DFG Reinhart Koselleck project and the Deutsche Forschungsgemeinschaft (DFG, German Research Foundation)—Project-ID 429529648—TRR 306 QuCoLiMa ('Quantum Cooperativity of Light and Matter'). WL thanks for the financial support by the 'China-Germany Postdoctoral Exchange Program'.

Data availability statement

The data generated and/or analysed during the current study are not publicly available for legal/ethical reasons but are available from the corresponding author on reasonable request.

ORCID iDs

Wenbing Li https://orcid.org/0000-0003-0427-6795
Dmitry Budker https://orcid.org/0000-0002-7356-4814

References

[1] Zhang J, Pagano G, Hess P W, Kyprianidis A, Becker P, Kaplan H, Gorshkov A V, Gong Z-X and Monroe C 2017 *Nature* **551** 601–4
[2] Blatt R and Roos C F 2012 *Nat. Phys.* **8** 277–84
[3] Johanning M, Braun A, Timoney N, Elman V, Neuhauser W and Wunderlich C 2009 *Phys. Rev. Lett.* **102** 073004
[4] Hilder J *et al* 2021 arXiv:2107.06368
[5] Blatt R and Wineland D 2008 *Nature* **453** 1008–15
[6] Cirac J I and Zoller P 1995 *Phys. Rev. Lett.* **74** 4091–4
[7] Brewer S M, Chen J S, Hankin A M, Clements E R, Chou C W, Wineland D J and Hume D B 2019 *Phys. Rev. Lett.* **123** 033201
[8] Keller J, Burgermeister T, Kalincev D, Didier A, Kulosa A P, Nordmann T, Kiethe J and Mehlstäubler T E 2019 *Phys. Rev.* A **99** 013405
[9] Huang Y, Guan H, Liu P L, Bian W, Ma L S, Liang K, Li T C and Gao K L 2016 *Phys. Rev. Lett.* **116** 013001
[10] Chou C W, Hume D B, Koelemeij J C, Wineland D J and Rosenband T 2010 *Phys. Rev. Lett.* **104** 070802
[11] Pyka K *et al* 2013 *Nat. Commun.* **4** 2291
[12] Ulm S *et al* 2013 *Nat. Commun.* **4** 2290
[13] Roos C F, Chwalla M, Kim K, Riebe M and Blatt R 2006 *Nature* **443** 316–9
[14] Nägerl H C, Roos C F, Leibfried D, Rohde H, Thalhammer G, Eschner J, Schmidt-Kaler F and Blatt R 2000 *Phys. Rev.* A **61** 023405
[15] Clark C R, Goeders J E, Dodia Y K, Viteri C R and Brown K R 2010 *Phys. Rev.* A **81** 043428
[16] Phillips W D 1998 *Rev. Mod. Phys.* **70** 721–41
[17] Chalony M, Kastberg A, Klappauf B and Wilkowski D 2011 *Phys. Rev. Lett.* **107** 243002
[18] Eschner J, Morigi G, Schmidt-Kaler F and Blatt R 2003 *J. Opt. Soc. Am.* B **20** 1003–15
[19] Diedrich F, Bergquist J C, Itano W M and Wineland D J 1989 *Phys. Rev. Lett.* **62** 403–6
[20] Poulsen G, Miroshnychenko Y and Drewsen M 2012 *Phys. Rev.* A **86** 051402
[21] Goodwin J F, Stutter G, Thompson R C and Segal D M 2016 *Phys. Rev. Lett.* **116** 143002
[22] Che H, Deng K, Xu Z T, Yuan W H, Zhang J and Lu Z H 2017 *Phys. Rev.* A **96** 013417
[23] Seck C M, Kokish M G, Dietrich M R and Odom B C 2016 *Phys. Rev.* A **93** 053415
[24] Thompson J D, Tiecke T G, Zibrov A S, Vuletić V and Lukin M D 2013 *Phys. Rev. Lett.* **110** 133001
[25] Feng L, Tan W L, De A, Menon A, Chu A, Pagano G and Monroe C 2020 *Phys. Rev. Lett.* **125** 053001
[26] Roos C F, Leibfried D, Mundt A, Schmidt-Kaler F, Eschner J and Blatt R 2000 *Phys. Rev. Lett.* **85** 5547–50
[27] Lechner R, Maier C, Hempel C, Jurcevic P, Lanyon B P, Monz T, Brownnutt M, Blatt R and Roos C F 2016 *Phys. Rev.* A **93** 053401
[28] Qiao M, Wang Y, Cai Z, Du B, Wang P, Luan C, Chen W, Noh H R and Kim K 2021 *Phys. Rev. Lett.* **126** 023604
[29] Cohen-Tannoudji C N and Phillips W D 1990 *Phys. Today* **43** 33–40
[30] Cohen-Tannoudji C N 1998 *Rev. Mod. Phys.* **70** 707–19
[31] Wineland D J, Dalibard J and Cohen-Tannoudji C 1992 *J. Opt. Soc. Am.* B **9** 32–42

[32] Chu S 1991 *Science* **253** 861–6
[33] Dalihard J and Cohen-Tannoudji C N 1989 *J. Opt. Soc. Am.* B **6** 2023–45
[34] Cirac J I, Blatt R, Parkins A S and Zoller P 1993 *Phys. Rev.* A **48** 1434–45
[35] Yoo S M and Javanainen J 1993 *Phys. Rev.* A **48** R30
[36] Birkl G, Yeazell J A, Rückerl R and Walther H 1994 *Europhys. Lett.* **27** 197–202
[37] Ejtemaee S and Haljan P C 2017 *Phys. Rev. Lett.* **119** 043001
[38] Joshi M K, Fabre A, Maier C, Brydges T, Kiesenhofer D, Hainzer H, Blatt R and Roos C F 2020 *New J. Phys.* **22** 103013
[39] Groot-Berning K *et al* 2019 *Phys. Rev.* A **99** 023420
[40] Stopp F *et al* 2019 *Hyperfine Interact.* **240** 33
[41] Haas R *et al* 2020 *Hyperfine Interact.* **241** 25
[42] Seiferle B *et al* 2019 *Nature* **573** 243–6
[43] Wineland D J, Monroe C, Itano W M, Leibfried D, King B E and Meekhof D M 1998 *J. Res. Natl Inst. Stand. Technol.* **103** 259–328